

A-Dependencies of Neutral Strange Particle Yields at 40 GeV/c \bar{p} -Nuclei Collisions

T.Grigalashvili, L.Chikovani, E.Ioramashvili, A.Javrishvili,
L.Khizanishvili, E.Mailian, M.Nickoladze, L.Shalamberidze

*Institute of Physics, Georgian Academy of Sciences,
Tamarashvili st.6, Tbilisi, 380077
Georgia*

*e-mail: eior@physics.iberiapac.ge
e-mail: etheri@iph.hepi.edu.ge*

Abstract

The interactions of \bar{p} with $D(2)$, $Li(7)$, $C(12)$, $S(32)$, $Cu(64)$ and $Pb(207)$ nuclei at 40 GeV/c were studied by RISC-streamer chamber spectrometer. The yields of K^0 mesons and Λ and $\bar{\Lambda}$ hyperons as functions of the target nucleus mass numbers are investigated. The experimental results are compared with model predictions using *FRITIOF* – 7.02 program package.

1 Introduction

Investigation of strange hadron formation at $\bar{p}p$ and $\bar{p}A$ interactions is of a great interest by several reasons. On the one hand, as in any other hadron-hadron collisions, the particles with nonzero strangeness can be formed only as a result of sea $s\bar{s}$ quarks production and of their subsequent hadronisation under condition of open strangeness. The study of such conditions gives the information on peculiarities of $s\bar{s}$ -pair formation and of their hadronisation mechanism.

On the other hand, availability of various data on strange particle formation permits to carry out comparative analysis of nonzero strangeness hadrons formation peculiarities at 32 GeV/c pp and $\bar{p}p$ interactions [1 – 3]. This allows to investigate the excess mechanism of strange mesons and baryons formation at $\bar{p}p$ collisions in comparison with pp interactions. The comparison of neutral strange particle formation gives evidence concerning the statement about pp and nonannihilated $\bar{p}p$ interactions equivalence [4].

The main contribution to the formation of new heavy quarks at ($\sqrt{s} < 20$ GeV) intermediate energies should give the light valence quarks and antiquarks annihilation subprocesses:

$$q_v\bar{q}_v \rightarrow g \rightarrow s\bar{s}, c\bar{c}, \dots$$

The large contribution of valence quarks annihilation to hard subprocesses is established quite reliably. For example, the yield of J/Ψ particles at 40 GeV/c $\bar{p}p$ interactions exceeds the yield at pp interactions ~ 12 times [5,6].

It was shown [3,7] that at $32 \text{ GeV}/c$ the main excess in the strange particle formation cross section at $\bar{p}p$ interactions is connected with $\bar{p}p$ annihilation process.

The mesons multiplicity increases with energy in $\bar{p}p$ annihilation processes, as at other hadron interactions [8], and the valence quarks and antiquarks of initial nucleons can be a part of different secondary mesons. For production of new $s\bar{s}$ pairs at $\bar{p}p$ annihilation can be spent a significant part of total energy as compared to pp interactions. This is caused by the fact that at pp interactions part of the total energy ($\sim 50\%$) is consumed by leading quarks-spectators which, according to existing knowledge, have a weak influence on the process of secondary hadrons formation [9].

But at $\bar{p}p$ annihilation all quarks and antiquarks of initial system can take part in the process of new $s\bar{s}$ pair formation. In quark-parton models, based on *QCD* principles, such mechanism of particle production at $\bar{p}p$ interactions is realized through annihilation or exchange of more than one $q\bar{q}$ pairs. In quark models based on the dual topological unitarization scheme $\bar{p}p$ annihilation is described by "three-chain" diagram [10] in which all three $q\bar{q}$ pairs take part in creation of new $s\bar{s}$ pairs.

Present article deals with the experimental study of the strange K^0 and Λ and $\bar{\Lambda}$ particles generation process at $40 \text{ GeV}/c$ $\bar{p}A$ (D, Li, C, S, Cu, Pb) interactions. The experimental material was obtained on Relativistic Ionization Streamer Chamber (*RISC*) in magnetic field. Our *RISC* setup ensured 4π angular coverage.

The experimental results will be compared with model predictions using *FRITIOF*-7.02 program package [11].

2 Experimental apparatus

The main part of *RISC* spectrometer is a large three-gap streamer chamber ($4.7 \times 0.9 \times 0.8 \text{ m}^3$ [12]) placed inside a magnetic field of about 1.5 T . The *HV*-pulses of $\pm 400 \text{ kV}$ and $\sim 20 \text{ ns}$ duration were produced and shaped by bipolar Marx generator and Blumlein line [13]. The chamber was filled with helium - neon gas mixture ($50\%Ne$ $50\%He$) at atmospheric pressure. The memory time of $(1 - 2) \mu\text{s}$ was achieved by a slight admixture of SF_6 . The sensitive volume of the chamber was viewed by 8 objectives, each equipped with two-stage image intensifier [14]. In addition, the triggered events could be directly controlled by means of television monitor.

The experiment was performed at Serpukhov proton synchrotron, using an unseparated beam of negatively charged particles with momentum of $40 \text{ GeV}/c$. The beam was composed of π^- and K^- and \bar{p} in $100 : 1.8 : 0.3$ ratio and had a momentum spread of $\Delta P/P \sim 1.5\%$.

The nuclear targets were placed in the visible volume of the chamber along the beam line with the spacing of 30 cm . The total thickness of all targets corresponded approximately to 12% of the proton absorption length. The elliptic target disks were mounted inside cylindrical mylar boxes.

A telescope consisting of two scintillation counters located behind the magnet of spectrometre served as a detector designed to single out the events of nonelastic interactions of beam particles in target. Signal of simultaneous starting operation of both counters was switched on for anticoincidence with the signal of incident particles, forming a "trigger of interaction" of corresponding particle in the target of spectrometre. On trigger signal the starting of streamer chamber took place. The detector excluded the events with negatively charged secondary particles for which the square of transferred 4 momentum equals in average to $t \leq 0.05 GeV/c^2$. At the same time a great part of the events of elastic scattering was excluded while the losses of non-elastic events were equal to 3 % according to the evaluations on the basis of the data of [15]. A more detailed description of the detector can be found in [16].

3 Data analysis

About 18000 frames of photographic film were scanned, and 7489 inelastic \bar{p} interactions with deuterium, lithium, carbon, sulphur, copper and lead nuclei were found. At the scanning stage all secondary two-prong stars V^0 (further refereed to as vees) were selected. They possibly are originated from the decays of neutral strange particles emitted from the primary interaction vertex. A double scan of the film ensured ~ 99 % efficiency in detecting the vees.

All tracks associated with the primary vertex, as well as the vertex and the tracks of a vee, were first measured and then geometrically reconstructed in the chamber volume. Events were retained for further analysis if:

- (a). the momentum error of the secondaries and of the V^0 - decay tracks is less then 10% and the residual (in space) does not exceed 1800 μm ;
- (b). the primary vertex is reconstructed within the target;
- (c). the V^0 's decay inside the fiducial volume. The cut imposes a target dependent minimum V^0 - path length and a maximum downstream length of 1m. The radius of the fiducial volume was chosen to ensure a minimum track length of 15 cm.
- (d). the space point reconstruction resolution in horizontal and vertical planes are $\Delta X \leq 0.1$ cm, $\Delta Y \leq 0.1$ cm, $\Delta Z \leq 0.4$ cm.

If the angle between the momentum of the parent neutral particle and the directions of two tracks of a vee was more then 6° , i.e. noncoplanary, this vee was rejected. (The mean uncertainty in the noncoplanarity angle is $\sim 0.7^\circ$). Vees rejected according to this criterion are mostly due to two-prong inelastic interaction or three-body decays of neutral particles.

A vee passing the above coplanarity selection was then kinematically fitted to each of four hypotheses ($K_S^0, \Lambda, \bar{\Lambda}, \gamma$) by the method of least squares for three degrees of freedom ($3DF - fit$). To resolve the V^0/γ - ambiguity, photon conversions were rejected by demanding $M(e^+e^-) > 30 \text{ MeV}/c^2$. This cut is sufficient to reject almost all γ 's and

does not remove V^0 's. To provide more reliable kinematical identification we retained only vees that satisfied the following criteria:

(a). For each track of a vee, the root-mean-square deviation of measured points from the fitted trajectory should not exceed 1.5 mm in the chamber volume.

(b). For each track of a vee, the relative momentum error $\Delta P/P \sim$ should be within 10%.

A vee was considered as an unambiguously identified if only one of the four hypotheses had a χ^2 value below 12 (see Fig.1). The mean values of χ^2 for identified particles proved to be

$$\begin{aligned} \langle \chi^2 \rangle_{K_S^0} &= 2.8 \pm 0.2, \quad \langle \chi^2 \rangle_{\Lambda} = 3.0 \pm 0.2, \\ \langle \chi^2 \rangle_{\bar{\Lambda}} &= 3.3 \pm 0.3. \end{aligned}$$

A vee was considered as an ambiguously identified if the condition $\chi^2 \leq 12$ was satisfied for two of the hypotheses. The ambiguity between Λ and K_S^0 was resolved in favor of K_S^0 , since the transverse momentum of the negatively charged particle from the vee exceeded $105 \text{ MeV}/c$ within the error. Observed ionization along both tracks of a vee was also used in identifying the parent that decayed. In total, nearly 5% of all detected neutral strange particles could not be unambiguously identified. These V^0 particles, determined ambiguously, were taken into account in calculations of output, but they did not participate in distribution of other kinematic characteristics.

Those neutral strange particles are indeed correctly identified that are demonstrated in Fig.(2 ÷ 4). The distributions of $\cos(\Theta^*)$ for identified strange particles are shown in Fig.2, where Θ^* is the angle between the directions of the V^0 and one of the decay products calculated in the V^0 rest frame for identified V^0 -s. The masses of K^0 and Λ and $\bar{\Lambda}$ candidates are plotted in Fig.3. The mean values are $\langle M_{K_S^0} \rangle = (0.490 \pm 0.003) \text{ GeV}$, $\langle M_{\Lambda} \rangle = (1.115 \pm 0.001) \text{ GeV}$ and $\langle M_{\bar{\Lambda}} \rangle = (1.116 \pm 0.001) \text{ GeV}$. The correlation between Podolansky-Armenteros parameter α and the negative decay product transverse momentum with respect to the vee direction is illustrated in Fig.4. The bands populated by neutral strange particles of each type are clearly seen.

To reconstruct the numbers of genuinely produced K^0 mesons, Λ hyperons and $\bar{\Lambda}$ hyperons, we introduced the required correction factors.

(1). The loss of events due to the limited dimensions of the chamber and the loss of particles in the target were taken into account by means of a geometric correction factor $\langle W_1 \rangle$, which depends on the target type since the mean multiplicity of emitted particles grows with increasing mass number of the target; as a result, the efficiency of determination of the vee vertex location deteriorates.

$$W_1 = 1 / [\exp(L_1/L_0) - \exp(L_n/L_0)]$$

L_1 is the radius of space in the vicinity of the target, where the observation because of V^0 peak is impossible of a large number of charged secondary particles.

L_n is the potential path.

L_0 is the length of free path of vee.

(2). Unobserved decay channels $K_S^0 \rightarrow \pi^0\pi^0$, $\Lambda \rightarrow n + \pi^0$ and $\bar{\Lambda} \rightarrow \bar{n} + \pi^0$, as well as the emission of long-lived K_L^0 mesons, were taken into account by means of $W_2(K^0) = 2.92 \pm 0.06$ and $W_2(\Lambda) = 1.56 \pm 0.01$ factors.

(3). The correction for the efficiency of scanning was included through factor $W_3 = 1.01$.

The overall correction factor W represents the product of the above mentioned three factors: $W = \langle W_1 \rangle W_2 W_3$. The values of the geometric correction $\langle W_1 \rangle_{K_S^0}$, $\langle W_1 \rangle_{\Lambda}$, $\langle W_1 \rangle_{\bar{\Lambda}}$ are presented in Table 1.

4 Experimental results

The A-dependencies of the yields of neutral strange particles ($K^0, \Lambda, \bar{\Lambda}$) were investigated in the following processes:

$$\bar{p}A \rightarrow K^0(K^0Y, K\bar{K}) + X \quad (1)$$

$$\bar{p}A \rightarrow \Lambda(\Sigma^0) + X \quad (2)$$

$$\bar{p}A \rightarrow \bar{\Lambda}(\bar{\Sigma}^0) + X \quad (3)$$

where Y is the hyperons ($\Lambda, \bar{\Lambda}, \Sigma^0, \Sigma^\pm$).

The experimental statistics, used in present article, is shown in Table 1. It includes the number of inelastic N_{int} interactions, among which V^0 events were found and the number of unambiguously identified neutral strange ($K_S^0, \Lambda, \bar{\Lambda}$) particles.

After making corrections for losses of V^0 events, connected with restrictions of mean path of particles in chamber and with nonobserved mode of decay of K^0 mesons and Λ and $\bar{\Lambda}$ hyperons, the total number of neutral strange particles for all studied nuclei were calculated. Thus, N_Λ includes also Λ hyperons, which have arisen as a result of Σ^0 decay.

On the basis of these data the average $\langle N_{K^0} \rangle$, $\langle N_\Lambda \rangle$ $\langle N_{\bar{\Lambda}} \rangle$ magnitudes presented in Table 2 were calculated for one inelastic interaction. The inclusive multiplicity $\langle N_{K^0} \rangle$ takes into account contributions both from the production of kaon pairs ($K^0\bar{K}^0, K^0K^-$ and \bar{K}^0K^+) and from associated kaon-hyperon production ($K^0\Lambda, K^0\Sigma^0, K^0\Sigma^-, \bar{K}^0\Sigma^+$ and $\bar{K}^0\bar{\Lambda}$). For their comparison the values calculated by Monte-Carlo method by program *FRITIOF* – 7.02 are presented for $\bar{p}A$ interactions. The table gives also the average magnitudes of neutral strange particle yields, obtained for $\bar{p}p$ interactions at 32 *GeV/c* momentum [3] and at 100 *GeV/c* momentum [17]. As it is shown from the Table the experimental results (for K^0 and Λ) slightly exceed the results of model. At increasing the mass number of target nucleus from deuterium to lead the average magnitudes of particle yields increase: $\langle N_{K^0} \rangle$ – 1.8 times, and

$\langle N_\Lambda \rangle - 2.5$ times; but $\langle N_{\bar{\Lambda}} \rangle$ remains constant within the error. The average magnitudes of Λ and $\bar{\Lambda}$ yields are equal both on hydrogen and on deuterium [3,17], as far as the C-symmetry at $\bar{p}p$ interactions assumes the equality of probabilities of Λ and $\bar{\Lambda}$ hyperons generation in events with identical multiplicity.

The A -dependencies of yields of K^0 mesons and Λ and $\bar{\Lambda}$ hyperons generated by reactions (1, 2, 3) are shown in Fig.5(a, b, c). The solid lines are the results of fitting the experimental data and dashed lines - the similar events calculated by *FRITIOF* - 7.02 program with power function $y = aA^\alpha$. The parameters (a, α) and χ^2 are presented in Table 3.

The behavior of yields of neutral strange particles with the increase of mass number is shown more clearly on the plot of dependence of relative $R_{V^0}^A$ yield (ratio of N_{K^0}, N_Λ and $N_{\bar{\Lambda}}$ for nucleus and corresponding values for hydrogen) and the ratio $R_{V^0} = \frac{\langle N_{K^0} \rangle}{\langle N_\Lambda \rangle}$ and $\frac{\langle N_{\bar{\Lambda}} \rangle}{\langle N_\Lambda \rangle}$ on $\langle \nu_{eff} \rangle$ (fig.6 a,b), where $\langle \nu_{eff} \rangle$ is the effective number of interactions in the frameworks of Glauber-Gribov model [18,19], and is determined as

$$\langle \nu_{eff} \rangle = \langle \nu \rangle / \langle \nu \rangle^a$$

and $\langle \nu \rangle^a = A\sigma_{\bar{p}p}^a / \sigma_{\bar{p}A}^a$ - is the correction for annihilation channels, where $\sigma_{\bar{p}p}^a = 5.6 mb$, is taken as the difference between sections of $\bar{p}p$ and pp interactions at 40 GeV/c [20].

The ratio of cross sections for annihilation and inelastic processes $\sigma_{\bar{p}A}^a / \sigma_{\bar{p}p}^{inel}$ calculated in the framework of Glauber-Gribov model [21] is given in Table 4.

All experimental results in Fig.4(a, b) are fitted by linear functions $y = a + b \langle \nu_{eff} \rangle$, the parameters of which are given in Tables 5.

Thus, within the experimental error $R_\Lambda^A = \frac{\langle N_\Lambda \rangle \bar{p}A}{\langle N_\Lambda \rangle \bar{p}p} \approx \langle \nu_{eff} \rangle$, and $R_{\bar{\Lambda}}^A = \frac{\langle N_{\bar{\Lambda}} \rangle \bar{p}A}{\langle N_{\bar{\Lambda}} \rangle \bar{p}p} \approx 1$. More rapid fall of $R_{K^0, \Lambda} = \frac{\langle N_{K^0} \rangle}{\langle N_\Lambda \rangle}$ is observed as compared to $R_{\bar{\Lambda}, \Lambda} = \frac{\langle N_{\bar{\Lambda}} \rangle}{\langle N_\Lambda \rangle}$.

5 Discussion of results

The obtained results were compared with those on *FRITIOF* - 7.02 based on quark-gluon-string model [11]. The universality of strings hadronisation is assumed in this model. This means the identity of multiple processes, taking place at inelastic pp and nonannihilation $\bar{p}p$ interactions, since the processes of annihilation and diffraction are absent in Lund model.

The model describes a wide sphere of phenomena from formation of charmed and beauty particles and effects of the fine gluons in hard processes to production of particles in soft interactions of hadrons with nucleons and nuclei [22-24].

In *FRITIOF* - 7.02 (version [25,26]) based on Lund model for soft hadron-hadron collisions the longitudinally-excited state is formed, i.e. the string between valence quarks (antiquarks) and diquarks (antidiquarks) of each hadron is stretched. The string is fragmented into hadrons by breakage. In the case of hadron-nuclear interaction

projectile hadron interacts more than once and obtained objects in excited states collide with nucleons before they passing through nucleus. Since the hadron fragmentation time is more than the internucleonic distance the string stretched by projectile particle does not have a time for fragmentation and continues to interact with nucleons of nucleus. As a result we have some number of strings fragmented into hadrons outside the nuclei.

The comparison of present experimental results with *FRITIOF* – 7.02 calculations shows a small difference in the neutral strange particle yields. This can be explained by the fact that $\bar{p}p$ annihilation is not taken into account in the model.

In experiments on heavy nuclei the value of N_{K^0} yield should be even more and the value of N_Λ yield should be approximately the same as in calculations since the probability of annihilation increases with increasing the atomic number [21,27].

Thus, the experimental results can be interpreted as follows: some differences in yields of K^0 mesons between the model and the experimental data is the consequence of the existence of annihilation channel at $\bar{p}A$ interactions. At the same time, a part of K^0 mesons (produced basically in annihilation channel) has time for secondary interactions in nucleus. This leads to the increase of Λ hyperon yield, as the threshold energy of Λ production is $\sim 2 \text{ GeV}/c$ [28].

The experiment shows that $\bar{\Lambda}$ hyperon yield, as was mentioned above, is practically independent of the atomic number, though the model predicts their small increase. Within the error their yield is equal to that of Λ hyperons for hydrogen and deuterium, and coincides with model prediction. This can be explained as follows:

The probability of annihilation processes increases with increasing the atomic number. But, on the one hand, this does not give the contribution to production of $\bar{\Lambda}$ hyperons. On the other hand, K^0 mesons, produced in annihilation channel, can not create $\bar{\Lambda}$ hyperons because of large threshold energy ($\sim 7 \text{ GeV}$ [28]).

The problems connected with other characteristics of $\bar{p}A$ interactions with production of neutral K^0 and Λ and $\bar{\Lambda}$ particles will be considered in further publications. Namely, the associated multiplicities of nucleons and negative mesons to the neutral strange particles; the inclusive characteristics of neutral strange particles and their dependencies on mass number of target nuclei will be investigated.

6 Conclusion

In the present article we have investigated the production of neutral strange particles in the processes of $\bar{p}A$ collisions at incident $40 \text{ GeV}/c$ momentum in wide range of nuclear targets (*D, Li, C, S, Cu, Pb*). The yields of K^0 mesons and Λ and $\bar{\Lambda}$ hyperons have been defined in dependence on mass number of nuclei in reactions (1, 2, 3).

The experimental results have been compared with theoretical predictions based on *FRITIOF* – 7.02 code. Following results should be mentioned:

1. The yield of K^0 mesons in process (1) grows as $\sim (0.20 \pm 0.01)A^{(0.141 \pm 0.007)}$.
2. The yield of Λ hyperons in process (2) grows as $\sim (0.054 \pm 0.005)A^{(0.22 \pm 0.01)}$.
3. The yield of $\bar{\Lambda}$ hyperons in process (3) remains constant within experimental error $\sim (0.07 \pm 0.01)A^{(-0.02 \pm 0.02)}$. Thus the relative yields $R_{\Lambda}^A = \frac{\langle N_{\Lambda} \rangle_{\bar{p}A}}{\langle N_{\Lambda} \rangle_{pp}} \approx \langle \nu_{eff} \rangle$ and $R_{\bar{\Lambda}}^A = \frac{\langle N_{\bar{\Lambda}} \rangle_{\bar{p}A}}{\langle N_{\bar{\Lambda}} \rangle_{pp}} \approx 1$, where $\langle \nu_{eff} \rangle$ is the effective number of interactions in nuclear.

4. Experimental values of K^0 and Λ particles yield slightly exceed the similar value predicted by *FRITIOF* – 7.02 code, but their A dependencies coincide within the error.

$\sim (0.179 \pm 0.004)A^{(0.155 \pm 0.003)}$ for K^0 mesons,

$\sim (0.054 \pm 0.003)A^{(0.202 \pm 0.007)}$ for Λ hyperons.

There is difference only in yields of $\bar{\Lambda}$ hyperons, where by *FRITIOF* – 7.02 a growth of $\sim (0.060 \pm 0.002)A^{(0.074 \pm 0.004)}$ is predicted.

7 Acknowledgement

We thank our colleagues in "RISC" Collaboration for their contribution to all stages of the experiment. We are indebted to N.N.Roinishvili and J.Manjavidze for enlightening comments and stimulating discussions.

This work was supported in part by the Academy of Sciences of Republic Georgia (Grant no. 2.11).

References

- [1] Bogolyubsky M.Iu. et al.:Yad.Fiz.48(1988)733
- [2] Bogolyubsky M.Iu. et al.:Yad.Fiz.43(1986)1199
- [3] Bogolyubsky M.Iu. et al.:Yad.Fiz.39(1984)1436
- [4] Bogolyubsky M.Iu. et al.:Yad.Fiz.50(1989)683
- [5] Corden M.J. et al.:Phys.Lett.B96(1980)411
- [6] Corden M.J. et al.:Phys.Lett.B98(1981)220
- [7] Ermolov P.F. et al.:Report IHEP,Protvino 83-126(1983)
- [8] Hanumajah B. et al.:Nouvo Cim.A68(1982)161
- [9] Anisovich V.V. et al.:KFKI(1982)36
- [10] Sukhatme U.P. et al.:Phys.Rev.Lett.45(1980)5
- [11] Nilsson-Almqvist B.,Stenlund E.:
Comput.Phys.Commun.43(1987)387
- [12] A.Javrichvili et al.:Nucl.Instrum.Methods177(1980)381
- [13] L.S.Vertogradov et al.:Prib.Tekh.Eksp.3(1978)31
- [14] E.M.Andreev et al.:Report JINR,Dubna I3-8550(1975)
- [15] S.P.Denisov, S.V.Donskov, Yu.P.Gorin et al.:Nucl.Phys.(1973), B61,62
- [16] E.M.Andreev et al.:Yad.Fiz.35(1982)700
- [17] Ward D.R. et al.:Phys.Lett.B62(1976)237
- [18] Sumiyoshi H. et al.:Report Univ.Tokio,INS-Rep-460(1982)
- [19] RISC collaboration.:Report JINR,Dubna E1-83-449(1983)
- [20] Batyunya B.V. et al.:Report JINR,Dubna E1-82-475(1982)
- [21] Boos E.G. et al.:Report JINR,Dubna E1-83-449(1983)
- [22] Anderson B. et al.:Phys.Rep.97(1983)31
- [23] Artu X.:Phys.Rep.97(1983)147

- [24] Anisovich V.V.,Shekhter V.M.:Nucl.Phys.B55(1973)455
- [25] Anderson B. et al.:Nucl.Phys.B281(1987)289
- [26] Anderson B. et al.:Nucl.Phys.B178(1981)242
- [27] Boos E.G. et al.:Z.Phys.C26(1984)43
- [28] Kladnitskaya E.N.:Particles and Nuclei 13(1982)669

Table Captions

Table 1. Sum of experimental statistics and geometric correction factors.

Table 2. Observed and predicted mean multiplicities of inclusive K^0 mesons and Λ and $\bar{\Lambda}$ hyperons.

Table 3. The parameters (a, α) and χ^2 of $y = aA^\alpha$ function for yields of neutral strange particles for experimental results and model predictions.

Table 4. The values of ratio of the annihilation and the inelastic cross sections $\sigma_{\bar{p}A}^a / \sigma_{\bar{p}p}^{inel}$ and corresponding $\langle \nu_{eff} \rangle$ for nuclei.

Table 5. The parameters (a, b) and χ^2 of $y = a + b \langle \nu_{eff} \rangle$ function for $R_{V^0}^A$ and R_{V^0} ratios for experimental results.

Figure Captions

Fig.1. Distribution of $P(\chi^2)$ for unambiguously identified particles.

Fig.2. Distribution of $\cos(\Theta^*)$ for unambiguously identified particles.

Fig.3. Distribution of invariant mass for identified particles (for $K_S^0 \rightarrow M(\pi^+\pi^-)$, for $\Lambda \rightarrow M(p\pi^-)$ and for $\bar{\Lambda} \rightarrow M(\bar{p}\pi^+)$).

Fig.4. Scatter plot of transverse momentum (p_t) of negative particles as a result of decays of K_S^0 and Λ and $\bar{\Lambda}$ versus Podolansky-Armenteros parameter (α).

Fig.5(a, b, c). Mean multiplicities of (a) inclusive K^0 mesons, (b) Λ and (c) $\bar{\Lambda}$ hyperons as function of the mass number of the target nucleus: (o) experimental data and (*) FRITIOF-7.02 predictions.

Fig.6(a, b). $R_{V^0}^A$ and R_{V^0} as functions of $\langle \nu_{eff} \rangle$ (see in the text).

Table 1. Sum of experimental statistics and geometric correction factors

A	N_{int}	$N_{K_S^0}$	N_{Λ}	$N_{\bar{\Lambda}}$	$\langle W_1 \rangle_{K_S^0}$	$\langle W_1 \rangle_{\Lambda}$	$\langle W_1 \rangle_{\bar{\Lambda}}$
D	1741	35	23	27	3.6 ± 0.4	3.5 ± 0.5	2.9 ± 0.3
Li	1149	36	22	20	2.4 ± 0.3	2.2 ± 0.4	2.0 ± 0.3
C	1053	30	16	16	2.8 ± 0.4	3.2 ± 0.4	2.0 ± 0.2
S	1197	47	36	24	2.6 ± 0.2	2.4 ± 0.2	2.3 ± 0.2
Cu	1346	42	34	14	3.6 ± 0.5	3.4 ± 0.4	2.8 ± 0.4
Pb	1003	29	28	17	3.8 ± 0.6	3.6 ± 0.4	2.1 ± 0.4

Table 2. Observed and predicted mean multiplicities of inclusive K^0 mesons and Λ and $\bar{\Lambda}$ hyperons.

Sample	$\langle N_{K^0} \rangle$	$\langle N_{\Lambda} \rangle$	$\langle N_{\bar{\Lambda}} \rangle$
$\bar{p}p$ [3] 32 GeV/c	0.21 ± 0.02	0.05 ± 0.01	0.06 ± 0.01
$\bar{p}p$ [17] 100 GeV/c	0.30 ± 0.02	0.07 ± 0.01	0.07 ± 0.01
Prediction	0.1902	0.0633	0.0654
$\bar{p}D$	0.24 ± 0.02	0.07 ± 0.01	0.07 ± 0.01
Prediction	0.1997	0.0585	0.0628
$\bar{p}Li$	0.25 ± 0.02	0.07 ± 0.01	0.06 ± 0.01
Prediction	–	–	–
$\bar{p}C$	0.27 ± 0.02	0.08 ± 0.02	0.06 ± 0.02
Prediction	0.2567	0.0941	0.0741
$\bar{p}S$	0.35 ± 0.02	0.13 ± 0.01	0.07 ± 0.01
Prediction	0.3148	0.1118	0.0752
$\bar{p}Cu$	0.38 ± 0.02	0.15 ± 0.02	0.05 ± 0.02
Prediction	0.3385	0.1240	0.0791
$\bar{p}Pb$	0.42 ± 0.03	0.17 ± 0.02	0.06 ± 0.02
Prediction	0.4069	0.1503	0.0911

Table 3. The parameters (a, α) and χ^2 of $y = aA^\alpha$ function for yields of neutral strange particles for experimental results and model predictions

Process	a	α	χ^2/NDF
$\bar{p}A \rightarrow K^0(K^0Y) + X$			
Experiment	0.20 ± 0.01	0.141 ± 0.007	1.3
Prediction	0.179 ± 0.004	0.155 ± 0.003	
$\bar{p}A \rightarrow \Lambda(\Sigma^0) + X$			
Experiment	0.054 ± 0.005	0.23 ± 0.01	0.7
Prediction	0.054 ± 0.003	0.202 ± 0.007	
$\bar{p}A \rightarrow \bar{\Lambda}(\bar{\Sigma}^0) + X$			
Experiment	0.07 ± 0.01	-0.02 ± 0.02	0.4
Prediction	0.060 ± 0.002	0.074 ± 0.004	

Table 4. The values of ratio of the annihilation and the inelastic cross sections $\sigma_{\bar{p}A}^a/\sigma_{\bar{p}A}^{inel}$ and corresponding $\langle \nu_{eff} \rangle$ for nuclei

A	H	D	Li	C	S	Cu	Pb
$\sigma_{\bar{p}A}^a/\sigma_{\bar{p}A}^{inel}$	0.15	0.17	0.21	0.24	0.30	0.35	0.44
$\langle \nu_{eff} \rangle$	1.0	1.1	1.4	1.6	2.0	2.5	3.0

Table 5. The parameters (a,b) and χ^2 of $y = a + b \langle \nu_{eff} \rangle$ function for $R_{V^0}^A$ and R_{V^0} ratios for experimental results

R	a	b	χ^2/NDF
$R_{K^0}^A = \frac{\langle N_{K^0} \rangle_{\bar{p}A}}{\langle N_{K^0} \rangle_{\bar{p}p}}$	0.57 ± 0.06	0.53 ± 0.02	0.2
$R_{\Lambda}^A = \frac{\langle N_{\Lambda} \rangle_{\bar{p}A}}{\langle N_{\Lambda} \rangle_{\bar{p}p}}$	-0.155 ± 0.004	1.07 ± 0.05	0.5
$R_{\bar{\Lambda}}^A = \frac{\langle N_{\bar{\Lambda}} \rangle_{\bar{p}A}}{\langle N_{\bar{\Lambda}} \rangle_{\bar{p}p}}$	1.2 ± 0.2	-0.06 ± 0.03	0.5
$R_{K^0, \Lambda} = \frac{\langle N_{K^0} \rangle}{\langle N_{\Lambda} \rangle}$	4.1 ± 0.8	-0.557 ± 0.004	0.2
$R_{\bar{\Lambda}, \Lambda} = \frac{\langle N_{\bar{\Lambda}} \rangle}{\langle N_{\Lambda} \rangle}$	1.4 ± 0.2	-0.36 ± 0.02	0.3

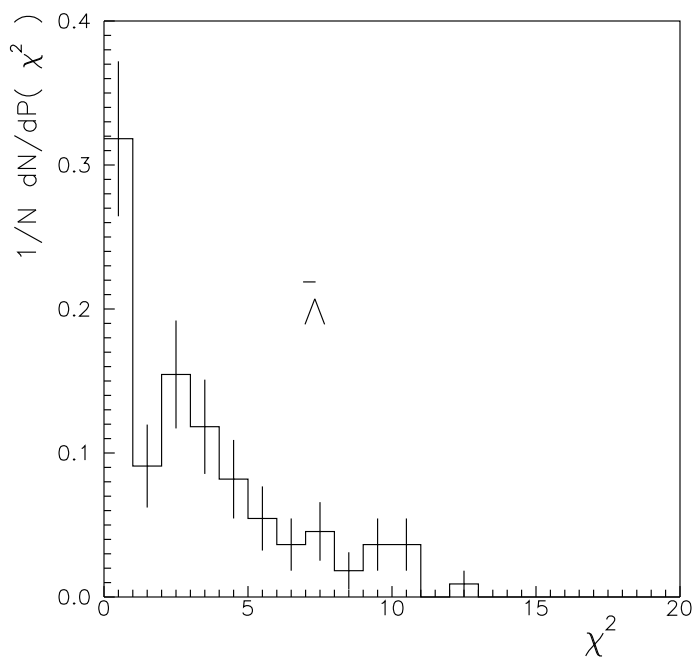
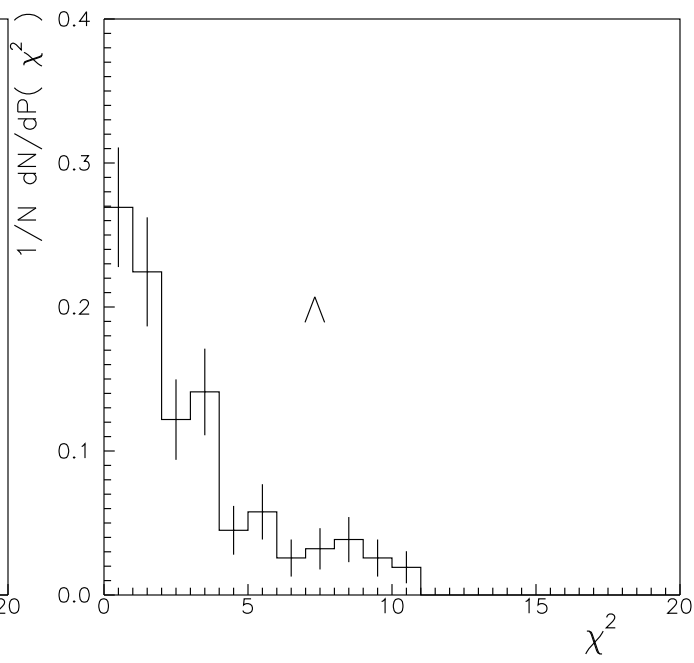
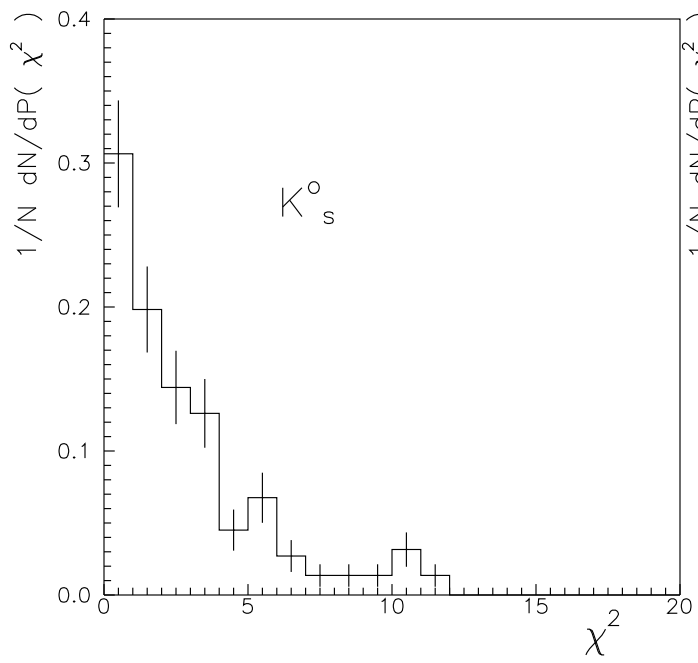


Fig.1

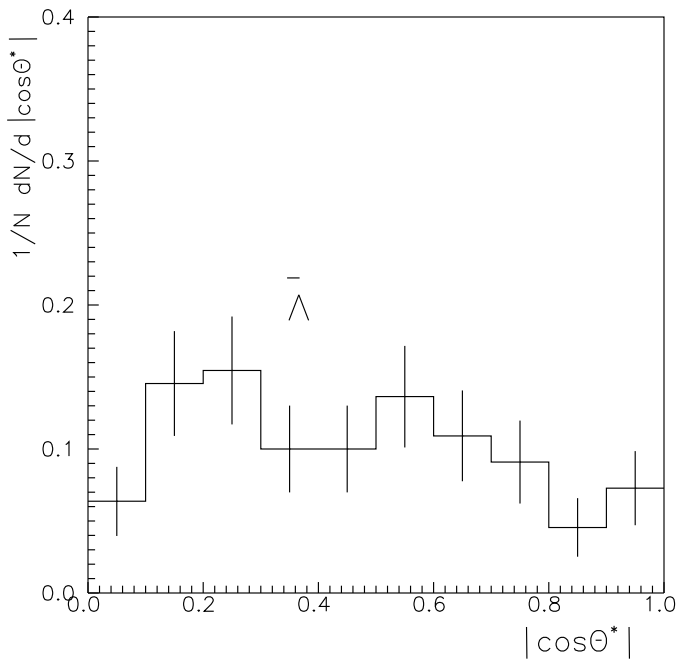
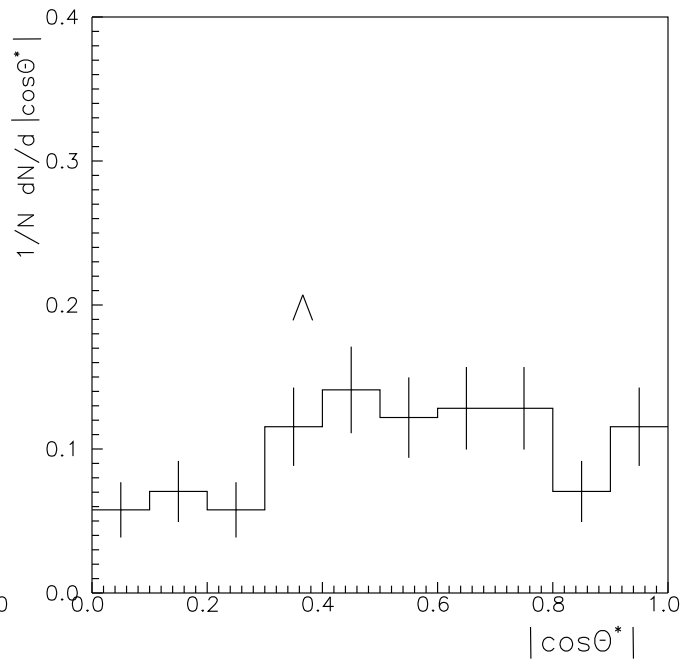
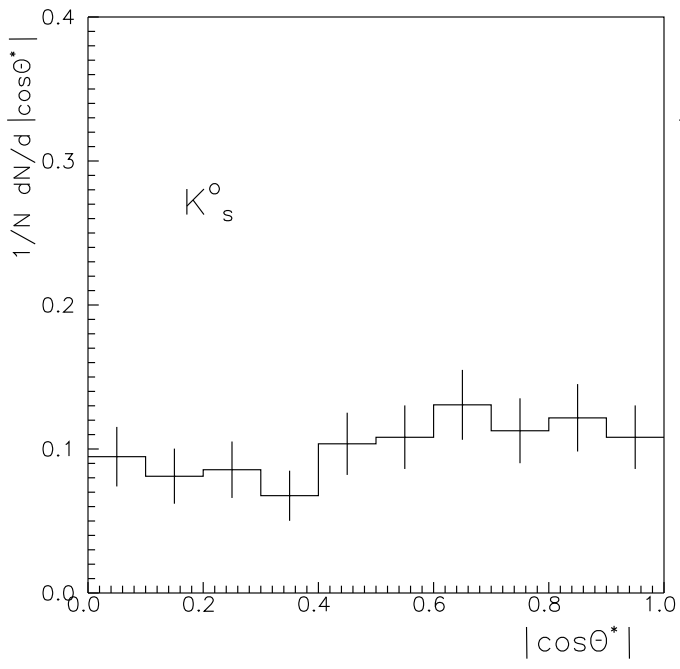
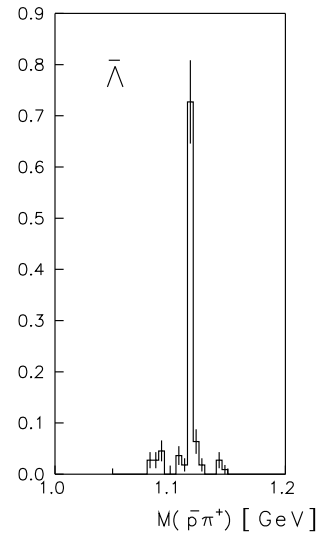
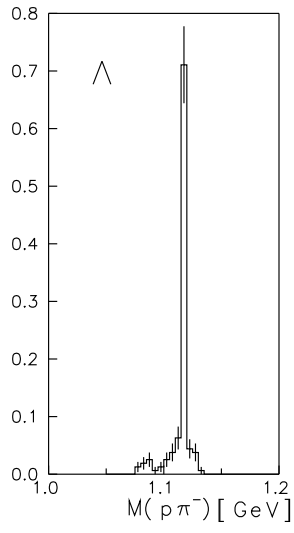
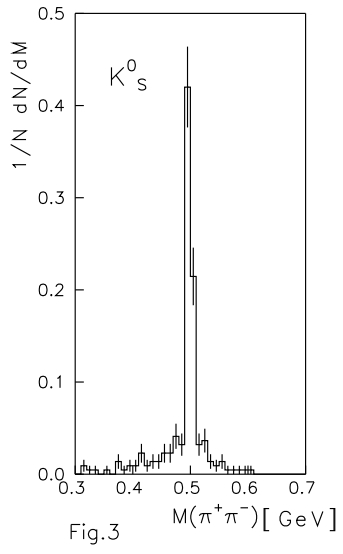


fig.2



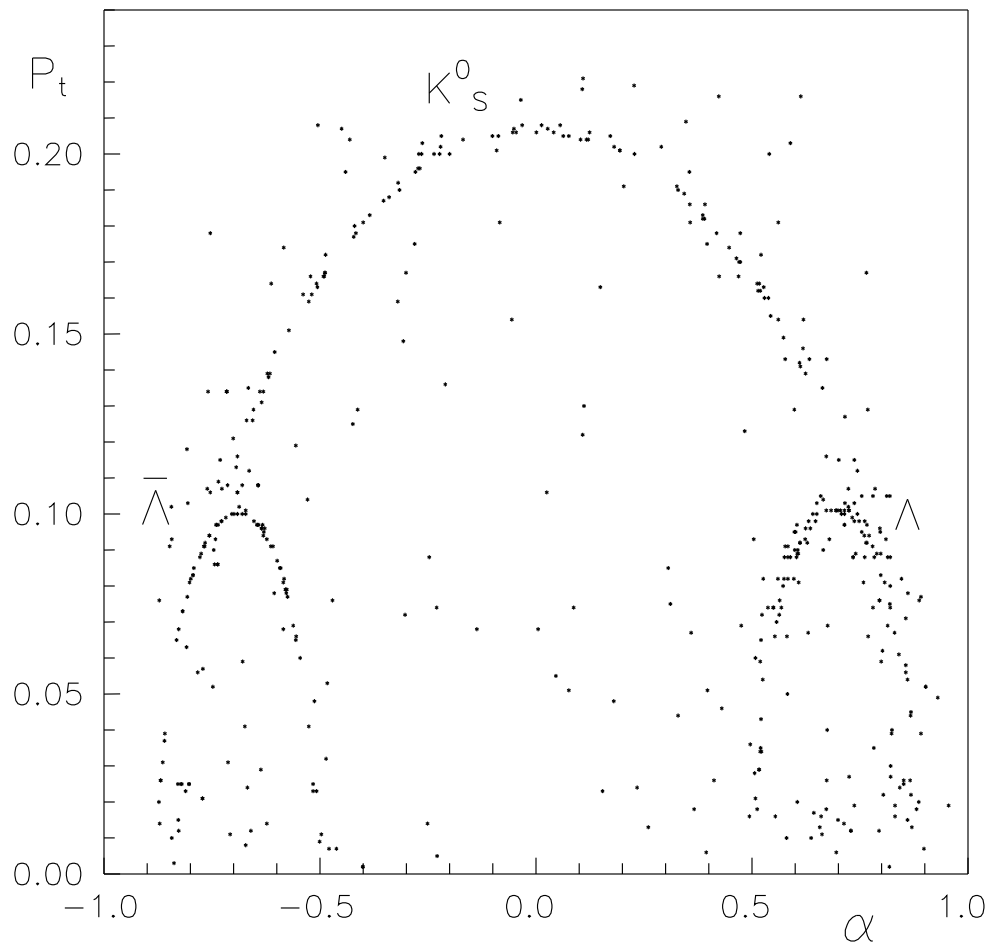


Fig.4

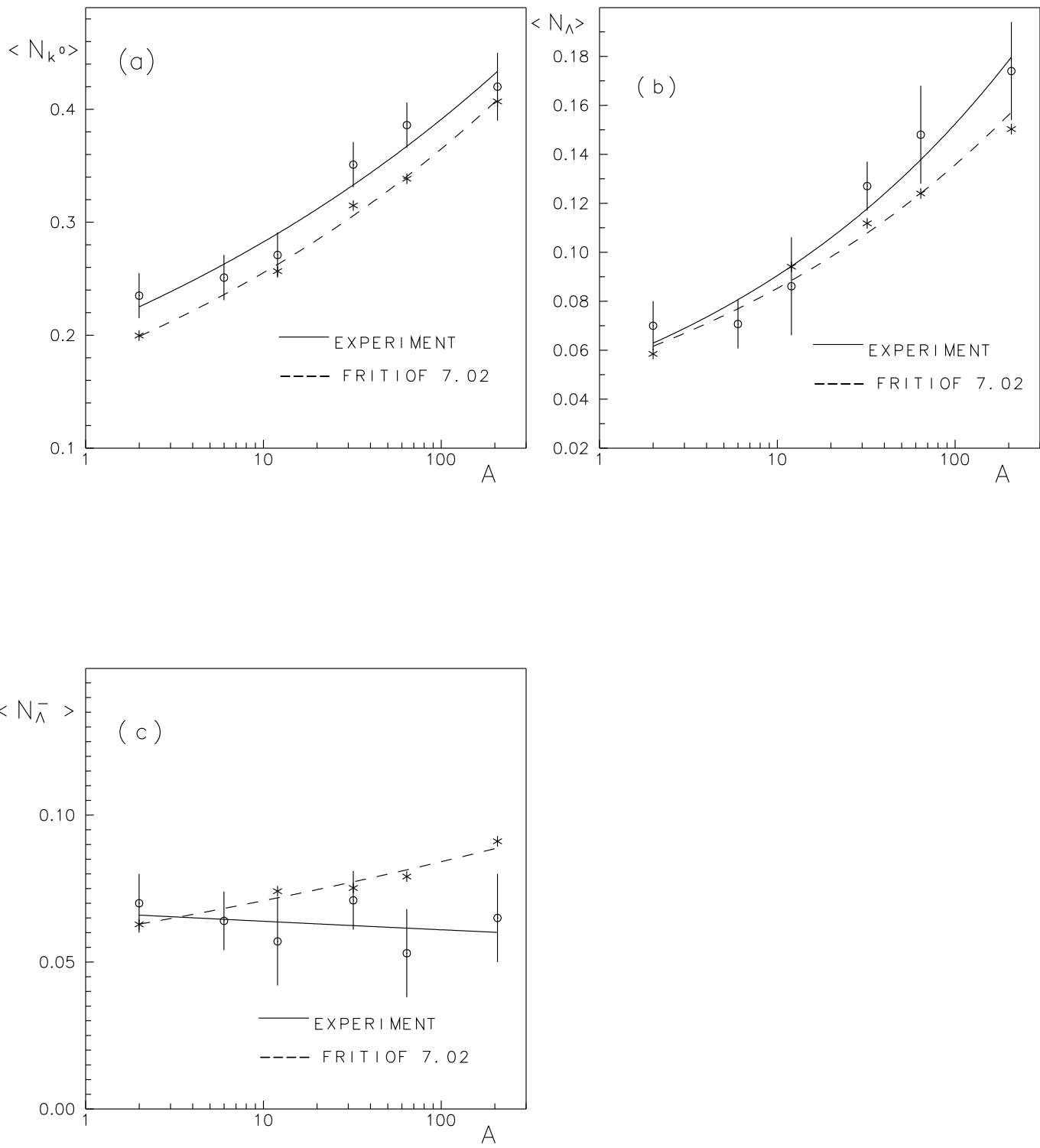


Fig.5

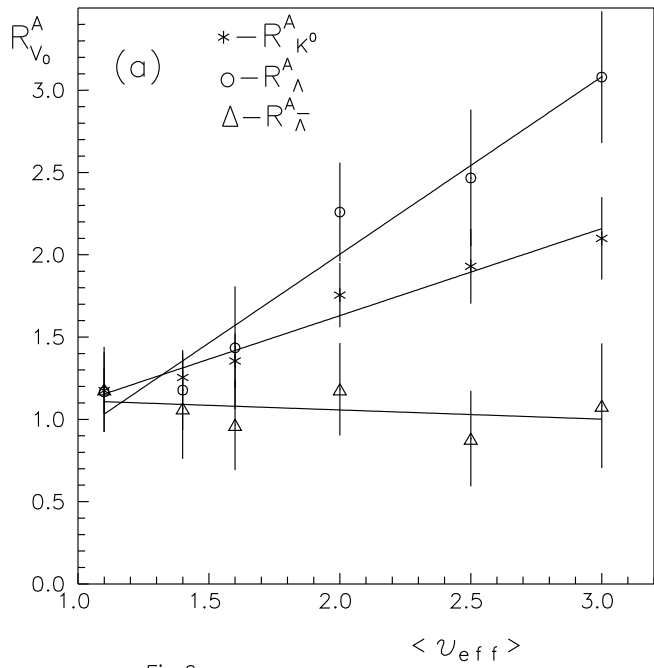


Fig.6

